processes

MDPI

Article

Simulation of Diffusion Processes in Chemical and Thermal Processing of Machine Parts

Kateryna Kostyk [1], Michal Hatala [2], Viktoriia Kostyk [3], Vitalii Ivanov [4], Ivan Pavlenko [5] and Darina Duplakova [2,*]

1 Department of Foundry, Educational and Scientific Institute of Mechanical Engineering and Transport, National Technical University Kharkiv Polytechnic Institute, Kyrpychova 2, 61002 Kharkiv, Ukraine; kateryna.kostyk@khpi.edu.ua
2 Department of Automobile and Manufacturing Technologies, Faculty of Manufacturing Technologies with a Seat in Presov, Technical University of Kosice, Bayerova 1, 080 01 Presov, Slovakia; michal.hatala@tuke.sk
3 Department of Computerized Mechatronic Systems, Tools and Technologies, Faculty of Machine Building, Donbas State Engineering Academy, Akademichna 72, 84313 Kramatorsk, Ukraine; vikakostik777@gmail.com
4 Department of Manufacturing Engineering, Machines and Tools, Faculty of Technical Systems and Energy Efficient Technologies, Sumy State University, Rymskogo-Korsakova St. 2, 40007 Sumy, Ukraine; ivanov@tmvi.sumdu.edu.ua
5 Department of Computational Mechanics named after V. Martsynkovskyy, Faculty of Technical Systems and Energy Efficient Technologies, Sumy State University, Rymskogo-Korsakova St. 2, 40007 Sumy, Ukraine; i.pavlenko@omdm.sumdu.edu.ua
* Correspondence: darina.duplakova@tuke.sk

Abstract: To solve a number of technological issues, it is advisable to use mathematical modeling, which will allow us to obtain the dependences of the influence of the technological parameters of chemical and thermal treatment processes on forming the depth of the diffusion layers of steels and alloys. The paper presents mathematical modeling of diffusion processes based on the existing chemical and thermal treatment of steel parts. Mathematical modeling is considered on the example of 38Cr2MoAl steel after gas nitriding. The gas nitriding technology was carried out at different temperatures for a duration of 20, 50, and 80 h in the SSHAM-12.12/7 electric furnace. When modeling the diffusion processes of surface hardening of parts in general, providing a specifically given distribution of nitrogen concentration over the diffusion layer's depth from the product's surface was solved. The model of the diffusion stage is used under the following assumptions: The diffusion coefficient of the saturating element primarily depends on temperature changes; the metal surface is instantly saturated to equilibrium concentrations with the saturating atmosphere; the surface layer and the entire product are heated unevenly, that is, the product temperature is a function of time and coordinates. Having satisfied the limit, initial, and boundary conditions, the temperature distribution equations over the diffusion layer's depth were obtained. The final determination of the temperature was solved by an iterative method. Mathematical modeling allowed us to get functional dependencies for calculating the temperature distribution over the depth of the layer and studying the influence of various factors on the body's temperature state of the body.

Keywords: steel; diffusion layer; hardening; surface hardness; nitriding; mathematical modeling

Citation: Kostyk, K.; Hatala, M.; Kostyk, V.; Ivanov, V.; Pavlenko, I.; Duplakova, D. Simulation of Diffusion Processes in Chemical and Thermal Processing of Machine Parts. *Processes* **2021**, *9*, 698. https://doi.org/10.3390/pr9040698

Academic Editor: Aneta Magdziarz

Received: 17 March 2021
Accepted: 14 April 2021
Published: 15 April 2021

1. Introduction

The widespread use of chemical-thermal treatment in various technology fields is explained by the fact that most machine parts and various mechanisms operate under wear, cavitation, cyclic loads, and corrosion at cryogenic or high temperatures, which maximum stresses occur in the surface layers of metal.

Chemical-thermal treatment of metals and their alloys for their surface hardening and protection against surface corrosion increases the reliability and durability of machine parts [1–5]. Parts such as bushings, pipes, washers, screws, gaskets, axles, shafts, gear

shafts, plungers, rods, crankshafts and camshafts, rings, spindles, screws, mandrels, rails, gear rings, semi-axles, gears, hydraulic cylinders, machine tool and turbine parts, as well as tools, punching tools, etc., need surface hardening. There are currently many surface hardening methods based on applying coatings or changing the surface condition. Among them, chemical-thermal treatment is widely used, which is used for alloys of both ferrous and non-ferrous metals.

The essence of the chemical-thermal treatment process is the saturation of the surface layers of the product with one or several elements at once combined with a certain heat treatment, which, depending on the type of chemical-thermal treatment, can be performed before and after saturation of the surface. Therefore, in chemical-thermal treatment, the structure and properties of the part's surface are due to both changes in the chemical composition of the surface and heat treatment.

The purpose of chemical-thermal treatment is to obtain a hard and wear-resistant surface of the part while maintaining a sufficiently plastic and viscous core matrix. Depending on the element that saturates the surface of the product, the following types of chemical-thermal treatment are distinguished:

- Cementation is carbon saturation. As shown in [6–8], cementation is particularly appropriate for achieving a large depth of steel products' carburization. The disadvantage of this method is the high labor intensity and poor variability of the conditions of carburization. The purpose of cementation is to create a stable, protective layer on the metal product's surface, increasing strength characteristics (including hardness and wear resistance). The main disadvantage of carburizing is the high complexity of the process.
- Nitriding is nitrogen saturation. Due to the increase in the specific volume of steel in the surface layer during nitriding and surface quenching, large internal compressive stresses occur. They help to reduce the tensile stresses from the external load during the operation of the part. As a result, the part's endurance, i.e., the ability to withstand a large number of repeated loads, increases, as shown in [9–12]. The nitriding process also has some technological advantages over carburizing: After nitriding, no quenching is required. The process temperature is 350–400 °C lower than during carburizing. As a result, the warping of the parts during nitriding is less. A serious disadvantage of nitriding is the long duration of this process. The nitriding cycle lasts up to two days. Besides, for nitriding, it is necessary to use expensive alloy steels, and therefore nitrided parts are obtained as 2–3 times more expensive than conventional ones.
- Nitrocementation (cyanidation) is the simultaneous saturation of carbon and nitrogen. The process of nitrocementation and cyanidation, as noted in [13–15], is carried out at relatively low temperatures, which contributes to less intensive wear of the equipment used and does not lead to significant deformations of the processed parts. Simultaneously, performing technological operations in such modes eliminates the need to cool the processed product to low temperatures. After cyanidation, the steel's austenitic structure becomes more stable, which improves the hardenability of individual sections of the material subjected to such treatment. It is particularly due to the cyanized material properties that low-alloy steels can be quenched in oil. The most significant drawback of such a type of nitrocementation as cyanidation is the high toxicity of the production components. For saturation with nitrogen and carbon, sodium and calcium cyanide salts are used, which are extremely toxic substances.
- Boriding is boron saturation. The most promising method of chemical-thermal treatment is boriding [16]. Boriding metals and alloys make it possible to obtain diffusion layers on their surface, which have many valuable operational properties. Thus, during the diffusion saturation of boron in steel structure, iron borides FeB and Fe_2B with high hardness are formed, contributing to increasing the wear resistance and heat resistance of products operating in various conditions. The main purpose of surface boriding is to increase the wear resistance of products' surfaces during operation in aggressive and abrasive environments at temperatures up to 800 °C.

- Silicification is the saturation of silicon. Silicification is carried out in powdered mixtures, gas, and liquid media. The silicified layer has high corrosion resistance in ordinary seawater and acid resistance in nitric, sulfuric, and hydrochloric acids [3]. Silicification also increases the heat resistance of steel to 700–750 °C. The disadvantage of silicifying steel is that it is almost impossible to obtain a uniform surface that will not have pores.
- Diffusion metallization is saturation with chromium, aluminum, etc. As shown in [17], the result of such treatment is a physical strengthening of the layer, an increase in its heat resistance, and an increase in resistance to the corrosion process—the surface is less worn during operation.

Regardless of the specific type of chemical-thermal treatment, three physical and chemical processes occur simultaneously during this treatment:

1. Dissociation [1] is the decomposition of the molecules of the saturating medium to obtain the necessary element in the active atomic (ionized) state.
2. Adsorption [18] is the absorption by the surface of the atoms (ions) of the saturating element, that is, the formation of a chemical bond between these atoms (ions) and the surface.
3. Diffusion [1,19] is the saturating element's movement into the metal's depth (product). In this case, a diffusion layer is formed, the concentration of elements in which differs from the initial one. So, the main process in chemical-thermal treatment is diffusion.

To form a layer on the surface of the appropriate composition and a certain depth, the part is placed in an environment rich in the element that should saturate the surface. The composition of the medium, the temperature, and the chemical-thermal treatment process's duration must be carefully controlled.

The slowest of these processes is diffusion, the rate of which is known to increase exponentially with increasing temperature. Therefore, the determining factor for obtaining the necessary depth of the diffusion layer is the temperature. The diffusion layer's depth also depends on the process's duration [1,3,7,8]. As shown in previous works [7,8], the diffusion rate at the penetration of diffusing atoms into the solvent lattice will be higher if solid solutions of introduction are formed during the interaction and much lower if solid solutions of substitution are formed. The diffusing element concentration on the surface depends on the influx of atoms of this element to the surface and the rate of diffusion processes, i.e., removing these atoms into the metal. The thickness of the diffusion layer depends on the heating temperature, the duration of exposure at saturation, and the diffusing element's concentration on the surface. The higher the diffusing element's concentration on the part's surface, the higher the layer thickness. The higher the temperature of the process, the greater the diffusion rate of the atoms, and consequently, the thickness of the diffusion layer increases.

Diffusion that causes phase recrystallization (with the formation of new phases) is often called reactive or reactive diffusion. This diffusion type occurs when steel is saturated with carbon, nitrogen [20,21], chromium, silicon, etc.

Diffusion in metals is based on an atomic process. Each free atom makes more or less random movements, that is, a series of jumps between different equilibrium positions in the lattice [22]. The concept of "diffusion" is applied not to individual atoms' movement but the macroscopic flow of substances. Macroscopic movements of matter are the result of a huge number of small movements of individual atoms. The driving force of diffusion is the gradient of the chemical potential, which various reasons can cause. For chemical-thermal treatment, the gradient of the chemical potential is determined by the concentration gradient.

Diffusion in a two- or multi-component system is possible only if one component is soluble in the other.

To form a representation of the diffusion process in a crystalline body (metal), a large number of possible diffusion mechanisms are proposed; there are four main mechanisms [19,22–24]:

1. Cyclical (exchange). When this mechanism is implemented, several atoms (three or more) located approximately in a circle move in concert so that the entire ring of atoms returns to one interatomic distance. A special case of the cyclic mechanism is the exchange mechanism, in which there is a direct exchange of places of two neighboring atoms. These mechanisms are unlikely in crystals with a structure with dense packing of atoms because they cause a strong distortion of the lattice at atoms' transition sites.
2. Crowdion mechanism. In this case, an extra atom appears in a more or less densely packed series of atoms. Each atom of this series, up to a distance of about ten interatomic distances from the extra atom, is displaced by some distance from the equilibrium position in the lattice. The crowdion configuration can move along this row. The distortion propagates along the line, and the displacement energy of the atoms is small.
3. Vacancy mechanism (diffusion by vacancies). In any crystal lattice, especially at elevated temperatures, there are vacancies. Vacancies open the way for easy diffusion due to the exchange of an atom with a vacancy. The transition of atoms to vacant positions is equivalent to moving in the opposite direction of atoms' movement. The vacancy mechanism is realized in self-diffusion and the formation of solid substitution solutions. The Kirkendahl effect is a convincing confirmation of the vacancy mechanism of diffusion [24], which is found in most pairs of metals with face-centered cubic and volume-centered cubic lattices and practically excludes the bulk and cyclic diffusion mechanism because the diffusion mobility of the atoms of the components (diffusion coefficients) is the same. In a vacancy mechanism, such equality is unnecessary: The exchange frequencies of atoms of different varieties with vacancies can differ. Many chemical-thermal treatment processes (cementation, nitriding, alitization, chrome plating, etc.) are caused by the diffusion of elements forming solid substitution solutions with iron [25–27]. Based on the material presented in these works, it can be concluded that the most difficult is a simple exchange mechanism of diffusion, and the most likely is a vacancy one. It is proved that the main mechanism of self-diffusion and diffusion in solid substitution solutions is the vacancy one. Elements such as carbon, nitrogen, aluminum, and chromium diffuse in iron by a vacancy mechanism. Porosity sometimes occurs in the diffusion layer, which in some cases can be explained by the Kirkendall effect.
4. Internode mechanism. In this case, the atom moves inside the crystal, jumping from one internode to another. Migration between the nodes is possible only when diffusion of small impurities of atoms forms solid solutions and a jump of relatively little displaced solvent atoms from their nodes in the lattice [23,28].

In industry, the most commonly used chemical-thermal treatment processes are based on the diffusion of nonmetals such as C, N, and B into iron. These elements have a small atomic radius and form solid solutions of introduction with iron. The diffusion of C, N, and B proceeds along with the interstitial mechanism. To perform the elementary act of diffusion, the free atom must overcome the energy barrier.

For the diffusion process to become possible, an energy fluctuation is needed. The atom from its neighbors obtains the excess energy because the atoms continuously exchange kinetic energy. Regardless of the average values of atoms' kinetic energy in metal, there will always be a certain number of atoms with increased or reduced energy. Individual atoms with energy fluctuations can overcome the energy barrier and jump from one equilibrium position to another.

The frequency of fluctuations exceeding Q determines the probability of jumps of an atom from one equilibrium position to another f_{m}. The relative time during which an atom has the energy needed to overcome the barrier is proportional to *exp(-Q/RT)*.

Hence, the value of f_{m} depends exponentially on the temperature.

The activation energy during diffusion by the vacancy mechanism is higher than by the interstitial one, and the diffusion mobility of atoms is lower. The deduction diffu-

sion movement also proceeds with less energy consumption in solid solutions than solid replacement solutions since they have ready-made vacancies in excess.

Diffusion in polycrystalline metals is much more intense than in single crystals. This is because diffusion is a structurally dependent process and is largely determined by the presence of defects in the crystal structure of metals [1,20,29]. As shown in these works, all structural defects, vacancies, grain boundaries and sub-boundaries, external surfaces, dislocations, etc., affect the diffusion mobility of atoms. During chemical-thermal treatment, both volume diffusion (in the volume of each grain), which contributes to diffusion flow, and diffusion along the grain boundaries are realized. The diffusion along the grain boundaries occurs at a much higher rate than in the grain volume. This is due to the fact that high-angle boundaries, regardless of their physical model, contain an increased concentration of vacancies and violations of the periodicity of the arrangement of atoms, which increases the probability of atomic transitions and reduces the activation energy of diffusion.

The development of the process of diffusion of atoms of the saturating medium leads to the formation of a diffusion layer, which is understood as the surface layer of the part material, which differs from the initial matrix material in chemical composition, structure, and properties. The material of the part's matrix under the diffusion hardened layer, which is not disturbed by the saturating medium's chemical action, is called the core.

The shortest distance from the saturation surface to the core is the total thickness of the diffusion layer. In the control of chemical-thermal treatment, the effective thickness of the diffusion layer is used, which is understood as the shortest distance from the saturation surface to the dimensional area characterized by the established limit nominal value of the base parameter.

The basic parameter of the diffusion layer is understood as the material's parameter. This test is the criterion for changing the quality depending on the distance from the saturation surface. As a basic parameter, either the concentration of the diffusion element, or properties, or a structural feature are taken.

The inner part of the diffusion layer adjacent to the core, determined by the difference between the total and effective thickness, is called the diffusion layer's transition zone.

2. Research Methodology

The gas nitriding technology was carried out in an electric shaft resistance furnace of the SSHAM-12.12/7 type. According to the furnace's technical requirements, nitriding of witness samples was carried out in an ammonia atmosphere [30].

Before nitriding, the products' surface was degreased by electrochemical method or washing in gasoline or in any other solvents to remove oil, emulsion, and other contaminants. Before nitriding, steels require pretreatment of the surfaces to be nitrided, with the help of which the oxide film must be removed, which prevents the diffusion of nitrogen deep into the metal. Nitriding of steels without preliminary depassivation leads to a decrease in the thickness of the layer, to its unevenness, and, as a result, to partial hardness. The oxidizing film is removed by digestion in an aqueous acid solution or introducing ammonium chloride or carbon tetrachloride into the furnace working space.

The following equipment was used for the gas nitriding process:

(a) Electric furnace SSHAM-12.12/7 with control panels.
(b) Rack with ammonia cylinders.
(c) Adsorber (silica gel desiccant).
(d) Disociometer, U-shaped pressure gauges, oil gate, taps.

The electric resistance furnace of the SSHAM-12.12/7 type is designed for gas nitriding. For nitriding, liquid ammonia of the first grade with a moisture content of up to 0.2% was used in cylinders under a pressure of up to 30 atm. Ammonia was supplied to the furnace from cylinders. Cylinders with ammonia were installed on a special rack. Flexible hoses connected all cylinders to the equipment. Liquid ammonia from the cylinders rushed into the adsorber. The ammonia pressure was monitored by a pressure gauge mounted on the

collector. The pressure on the first stage of the gearbox should be within 2 atm. Gaseous ammonia through the collector entered the ammonia two-stage gearbox DR-IA, which is designed to reduce and maintain pressure in the pipeline system.

The adsorber is designed to drain the ammonia that entered the furnace. An adsorber is an empty cylinder equipped on both sides with flanges that are bolted to it. A mesh basket with a moisture separator-silica gel was placed inside the adsorber. Ammonia entered the adsorber through the lower nozzle, passed through the silica gel and drained through the lower nozzle, then entered the system. The dissociometer is designed to determine the degree of dissociation of ammonia and is a capacity graded by 100 divisions. The principle of operation of the device is based on the property of ammonia to dissolve in water. Above and below, the container was closed by cranes. One branch of the lower two-way tap is connected to the liquid discharge line into the sewer, and the second is connected to the gas discharge line into the air (through the oil gate).

To determine the degree of dissociation of ammonia, both taps were opened so that the gases leaving the furnace passed through the dissociometer. After 40–60 s, the lower tap was closed, and the other was turned so that the dissociometer was filled with water. Ammonia dissolved in water, but nitrogen and hydrogen did not dissolve. The degree of dissociation of ammonia was determined by the volume filled with gases. During gas nitriding of steel witness samples at nitriding temperatures, the ammonia dissociation degree was in the range of 30–50%.

The specimens were placed in the device so that they do not touch each other to prevent areas on the surfaces of the samples or products diffusion-less hardening, and to ensure a free contact with the surface of the metal to be nitrided, the decay products of ammonia, which play an important role in the processes of diffusive saturation. After that, the witness samples with the details were immersed in the furnace and hermetically sealed.

We purged the muffle furnace until complete air extraction, which from there was mounted on the dissociate (complete filling of dissociating water indicates the absence of air in the oven), then the oven was turned on. The purge period was 30–60 min.

Gas nitriding was carried out according to the following technological scheme: Pre-annealing, improvement (quenching with high tempering), degreasing, direct gas nitriding for 20, 50, and 80 h, slow cooling of the products together with the furnace to a temperature of 200 °C, followed by cooling in calm air.

The experiments were carried out in the temperature range of 400–700 °C in increments of 10 °C.

To obtain a mathematical model, the temperature range 500–560 °C was selected. Namely, the points indicated in Tables 1 and 2 (500, 530, 560 °C), where the average values of the experimentally obtained data after gas nitriding, are presented.

Table 1. Average values of the experimentally obtained data of the nitrided layer depth after gas nitriding, microns.

Duration of Gas Nitriding, h	The Temperature of Nitriding, °C		
	500	**530**	**560**
20	40	100	190
50	400	500	540
80	570	610	650

The resulting model of the depth of the nitrided layer, depending on the normalized values of temperature and duration of chemical-thermal treatment, has the form of a polynomial of the second degree with the following values of coefficients:

$$y = 402.22222 + 61.679 \cdot x_1 + 246.716 \cdot x_2 - 11.727 \cdot x_1^2 - 116.727 x_2^2 - 17.5 \cdot x_1 \cdot x_2 \quad (1)$$

Table 2. Average values of the experimentally obtained data of the surface hardness of steel 38Cr2MoAl after gas nitriding, GPa.

Duration of Gas Nitriding, h	The Temperature of Nitriding, °C		
	500	**530**	**560**
20	7.5	8.5	6.5
50	10	9.5	8
80	9	9.2	7.5

3. Results and Discussion

The problem of controlling the diffusion process to obtain certain qualitative characteristics of the hardened layer can be briefly formulated as the problem of ensuring a certainly given distribution of the nitrogen concentration *C (x, τ)* over the depth of the diffusion layer *x* from the surface of the product [8].

The diffusion stage model is used under the following assumptions:

1. The diffusion coefficient of the saturating element primarily depends on the temperature change.
2. The metal surface is instantly saturated to equilibrium concentrations with the saturating atmosphere.
3. The surface layer and the entire product are heated unevenly. The product temperature is a function of time and coordinates *t (x, τ)*.

The following partial differential equations represent the mathematical model:

The diffusion equation describing the process of diffusion saturation [20,24]:

$$\frac{\partial C(x,\tau)}{\partial \tau} = \frac{\partial}{\partial x}\left\{ D[t(x,\tau)]\frac{\partial C(x,\tau)}{\partial x} \right\}; \quad (2)$$

The equation of non-stationary thermal conductivity describing the process of temperature distribution in the product [20,24]:

$$C_V(x)\frac{\partial t}{\partial \tau} = \frac{\partial}{\partial x}\left[\lambda(x)\frac{\partial t}{\partial x} \right] \quad (3)$$

where $D[t(x,\tau)]$—the diffusion coefficient;

$C_V(x)$—heat capacity of a unit of volume;

$\lambda(x)$—the coefficient of thermal conductivity, which is a physical parameter of a substance and characterizes a material's ability to conduct heat. It is also a proportionality coefficient in the Fourier law equation.

Boundary conditions for concentration:

$$C(0,\tau) = C_0(\tau) \quad (4)$$

$$\frac{\partial C(L,\tau)}{\partial x} = 0. \quad (5)$$

The initial conditions:

$$C(x,0) = 0. \quad (6)$$

To solve problem (2), using boundary and initial conditions (4)–(6), it is necessary to determine the temperature distribution *t (x,τ)* over the depth of the diffusion layer from Equation (3).

For this purpose, the problem of non-stationary thermal conductivity in an inhomogeneous body was considered. To simplify the problem, we assumed that the temperature is a function of the x coordinate and time τ:

$$t = f(x, \tau), \text{ if } \frac{\partial t}{\partial y} = \frac{\partial t}{\partial z} = 0. \quad (7)$$

The temperature in the body changed only in the direction perpendicular to the surface. Simultaneously, the greatest temperature difference per unit length occurred in the direction of the normal n to the surface. The temperature gradient is a vector normal to the surface of the product whose value has the opposite sign, indicating that the temperature drop is the limit of the ratio of temperature change Δt and the distance between the isotherms at the normal Δn:

$$lim\left(\frac{\Delta t}{\Delta n}\right)_{\Delta n \to 0} = \frac{\partial t}{\partial n} = gradt. \quad (8)$$

According to Fourier's law, the amount of heat transferred in a solid is proportional to the drop in temperature, time, and cross-sectional area perpendicular to the direction of heat propagation. The amount of heat transferred concerning a unit of area and a unit of time is recorded:

$$q = -\lambda \, grand \, t \quad (9)$$

Equation (9) is a mathematical expression of heat propagation's basic law using solids' thermal conductivity. The temperature gradient is assumed to be in the flow direction, and the conducting plane is normal to the flow direction. The heat flux q is the amount of heat transferred per unit of time through a unit of surface. This value is a vector whose direction coincides with the direction of heat propagation and is opposite to the temperature gradient direction, as indicated by the minus sign in Equation (9).

Let us consider the case of when the heat is transferred through a solid, boundary conditions of the second kind are set on one of its surfaces and of the third kind on the other. In this case, the heat flux values are set for each point on the body's surface and at any time. Analytically, this can be represented as follows:

$$q_0 = f(x, \tau) \quad (10)$$

where q_0—the density of heat flow on the surface of the body.

We assume that the density of the heat flow over the surface and over time remains constant:

$$q_0 = const, \; if \; x = 0$$

On the other surface of the solid, limit conditions of the third kind are given. In this case, the ambient temperature t_0 and the law of heat exchange between the body's surface and the environment are set. The ultimate condition of the third kind of the law describes the heat transfer between the surface and the environment in the process of cooling the body according to Newton's law-Richman, following which the amount of heat given to a unit of body surface per unit time is proportional to the temperature difference between the surface of the body $t_{x=0}$ and the environment t_0 ($t_{x=0} > t_0$):

$$q = \alpha(t_{x=0} - t_0) \quad (11)$$

where α is the proportionality coefficient, called the heat transfer coefficient, which characterizes the intensity of heat exchange between the surface of the body and the environment. Numerically, it is equal to the amount of heat given (or perceived) by a unit of surface per unit of time when the temperature difference between the body's surface and the environment is equal to one degree.

According to the law of conservation of energy, the amount of heat that is removed per unit area per unit time due to heat loss must equal the heat supplied to the unit surface per unit time due to heat conduction from the inner volume of the body:

$$\alpha(t_{x=0} - t_0) = -\lambda\left(\frac{\partial t}{\partial n}\right)_{x=0} \tag{12}$$

Thus, the body is exposed to a uniformly distributed heat source with power q_0 over the surface $x = 0$ and convective heat exchange with the environment through the surface $x = L$.

We assume that the diffusion layer's thermophysical characteristics are functions of coordinates, and the main material of the product has constant characteristics. There are no internal sources in the body ($q_v = 0$).

Then this problem is described by Equation (3) under the following initial conditions:

$$t(x, 0) = t_0 \tag{13}$$

and mixed boundary conditions of the second and third kind:

$$-\lambda(0)\left.\frac{\partial t}{\partial x}\right|_{x=0} = q_0 \tag{14}$$

$$-\lambda(L)\left.\frac{\partial t}{\partial x}\right|_{x=L} = \alpha(\left.t\right|_{x=L} - t_0) \tag{15}$$

To solve the problem (3), (13)–(15), the differential-difference method is applied. A uniform grid over the variable τ is introduced:

$$W_\tau = \left\{\tau_i = (i-1)h_\tau; i = 1, 2, 3, \ldots M; h_\tau = \frac{\tau_M}{M-1}\right\}$$

By replacing $\frac{\partial t}{\partial x}$ with a different relation, the original problem can be mapped to a differential-difference problem:

$$\frac{\partial}{\partial x}\left[\lambda(x)\frac{\partial t_i}{\partial x}\right] = \frac{C_V(x)}{h_\tau}(t_i - t_{i-1}) \tag{16}$$

$$-\lambda(0)\left.\frac{\partial t_i}{\partial x}\right|_{x=0} = q_0; \tag{17}$$

$$-\lambda(L)\left.\frac{\partial t_i}{\partial x}\right|_{x=L} = \alpha(\left.t_i\right|_{x=L} - t_0); \tag{18}$$

We present the thermophysical characteristics of an inhomogeneous body (the diffusion layer and the base material) in the form:

$$P(x) = P_0 + \lim_{N\to\infty}\sum_{n=1}^{N}(P(x_n) - P(n-1))\delta(x - x_n)h_n \tag{19}$$

where $P(x) = \begin{cases} \lambda(x) \\ C_V(x) \end{cases}$; $P_0 = \min p(x_n)$; h_n—the characteristic linear size of the inclusion with the characteristics $p(x_n), \delta(x - x_n)$—a Dirac function that allows you to record the point impact and heat intensity.

The number of points N is selected depending on the characteristics of the product material (the geometry of the inhomogeneous layer, inclusions, the number of points in which the values of thermal characteristics are known).

Regarding the temperature value obtained in the previous step $t_{i-1}(x)$, let us represent it in the form:

$$t_{i-1}(x) = \lim_{N\to\infty} \sum_{n=1}^{N} t_{(i-1)n} x_n \delta(x - x_n) h_n \tag{20}$$

Thus, the problem (16)–(18) taking into account (19), (20) is transformed into the form:

$$\frac{d^2 t_i}{dx^2} - \gamma^2 t_i = -\sum_{n=1}^{N} \left[\frac{(\lambda_n - \lambda_{n-1}) h_n}{\lambda_0} \cdot \frac{dt_{in}}{dx} \delta(x - x_n) - \frac{C_{Vn} - C_{V0}}{\lambda_0 h_\tau} h_n t_{in} \delta(x - x_n) + \frac{C_{Vn} h_n}{\lambda_0 h_\tau} t_{(i-1)n} \delta(x - x_n) \right], \tag{21}$$

where

$$\lambda_n = \lambda(x_n), t_{in} = t_i(x_n)$$

$$\gamma^2 = \frac{C_{V0}}{\lambda_0 h_\tau};$$

$$q_0 = -\lambda_1 \frac{dt_{i1}}{dx} \tag{22}$$

$$-\lambda_{DL} \frac{dt_{iN}}{dx} = \alpha(t_{iDL} - t_0) \tag{23}$$

The general solution of equation (21) has the form:

$$t_i = C_1 e^{\gamma x} + C_2 e^{-\gamma x} - \frac{1}{2\lambda_0 h_\tau} \sum_{n=1}^{N} h_n e^{-\gamma|x - x_n|} \times \left[(\lambda_n - \lambda_{n-1}) \frac{dt_{in}}{dx} \mathrm{sng}(x - x_n) + \frac{C_{vn} - C_{v(n-1)}}{\gamma} t_{in} - \frac{C_{vn}}{\gamma} t_{(i-1)n} \right], \tag{24}$$

where $\mathrm{sng}(x - x_n) = \begin{cases} 1, x \geq x_n, \\ -1, x < x_n \end{cases}$ —this is a piecewise constant function.

Having satisfied the boundary conditions (26), (27), we define the integration constants C_1 and C_2

$$\frac{dt_i}{dx} = \gamma\left(C_1 e^{\gamma x} + C_2 e^{-\gamma x}\right) + \frac{\gamma}{2\lambda_0 h_\tau} \sum_{n=1}^{N} h_n e^{-\gamma|x - x_n|} \times$$

$$\times \mathrm{sng}(x - x_n) \left[(\lambda_n - \lambda_{n-1}) \frac{dt_{in}}{dx} \mathrm{sng}(x - x_n) - \frac{C_{vn} - C_{v(n-1)}}{\gamma} t_{in} - \frac{C_{vn}}{\gamma} t_{(i-1)n} \right]$$

or

$$\frac{dt_i}{dx} = \gamma\left(C_1 e^{\gamma x} + C_2 e^{-\gamma x}\right) + \frac{\gamma}{2\lambda_0 h_\tau} \sum_{n=1}^{N} h_n e^{-\gamma|x - x_n|} \times \left\{ (\lambda_n - \lambda_{n-1}) \frac{\partial t_{in}}{\partial x} + \frac{\mathrm{sng}(x - x_n)}{\gamma} \left[\left(C_{vn} - C_{v(n-1)} \right) t_{in} - C_{vn} t_{(i-1)n} \right] \right\} \tag{25}$$

We get:

$$t_i = \frac{2q_0}{\lambda_1 \gamma z} (\alpha - \lambda_{DL}\gamma) e^{-\gamma L} \mathrm{ch}\gamma x - \frac{2\alpha T_0}{z} \mathrm{ch}\gamma x + \frac{1}{2\lambda_0 h_\tau} \times$$

$$\times \sum_{n=1}^{N} h_n \left\{ (\lambda_n - \lambda_{n-1}) \frac{dt_{in}}{dx} \left[e^{-\gamma(x - x_n)} + \frac{4(\lambda_{DL} - \gamma)}{z} e^{-\gamma L} \mathrm{ch}\gamma x_n \mathrm{ch}\gamma x \right] + \right.$$

$$+ \left[\left(C_{Vn} - C_{V(n-1)} \right) t_{in} - C_{Vn} t_{(i-1)n} \right] \times$$

$$\left. \times \left[(1 - \mathrm{sng}(-x_n)) \frac{4(\lambda_{DL} - \gamma)}{z\gamma} e^{-\gamma L} \mathrm{ch}\gamma x_n \mathrm{ch}\gamma x + \frac{\mathrm{sng}(-x_n)}{\gamma} \right] \right\}$$

where

$$\mathrm{sng}(x) = \begin{cases} 1, x \geq 0, \\ -1, x < 0; \end{cases}$$

$$z = e^{-\gamma L}(\lambda_{DL}\gamma - \alpha) - e^{-\gamma L}(\lambda_n \gamma + \alpha) \tag{26}$$

Differentiating Equation (26) by x and taking $x = x_n (n = 1, 2, \ldots, N)$ we obtain together with (26) a system of algebraic equations for determining t_{in} and $\frac{dt_i}{dx}$, which is solved by the iterative method.

On the example of the gas nitriding process, according to (34), taking into account the found values t_{in} and $\frac{dt_i}{dx}$, calculations are performed, and results are obtained, which are shown in Figure 1.

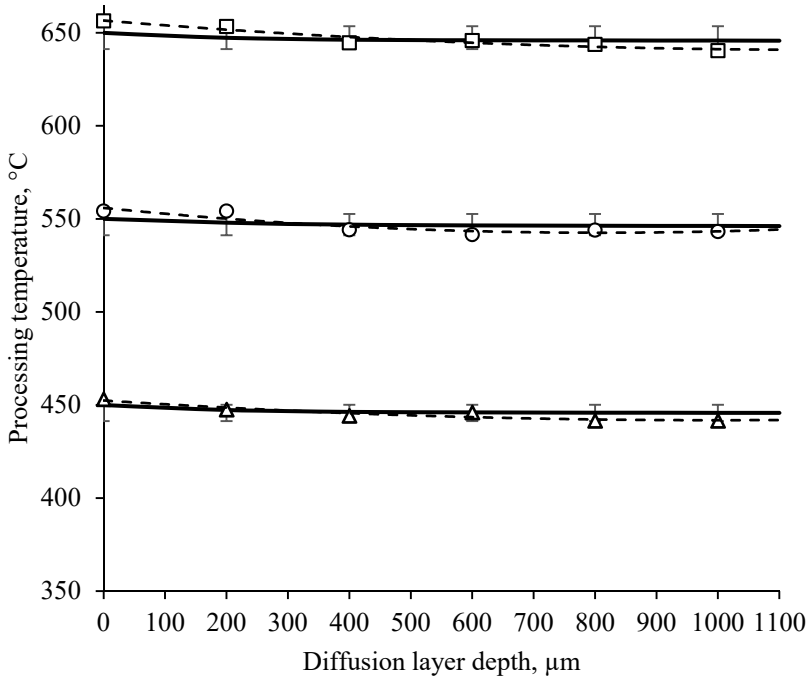

Figure 1. Temperature distribution over the depth of the diffusion layer at different processing temperatures.

To test the model outside the simulation range, the temperatures shown in Figure 1 were selected (450, 550, 650 °C). This allowed us to conclude the reliability (adequacy) of the mathematical model both in the modeling range (550 °C) and outside the modeling range (450 and 650 °C).

The diffusion layer's temperature distribution's magnitude and nature depend on the supplied heat's power, the heat source's duration, and influence. With an increase in the gas nitriding temperature, the curves' nature almost does not change (Figure 1). An intense temperature drop is observed from the samples' surface to about 400 microns of the diffusion layer. For the temperature range 450–650 °C, this temperature drop is 3 °C. From 400 microns, the temperature distribution deep into the samples is very smooth. This temperature distribution may be related to the diffusion layers' structural features and the different saturating element concentrations in depth. The dotted line in Figure 1 shows approximations of the mean values of the experimentally obtained data. The error of the obtained theoretical and experimental data does not exceed 3–5%. There is a pattern that the experimentally obtained data are slightly higher than the theoretically obtained ones up to 400 microns, and vice versa at a greater depth of 400 microns.

The research study [31], devoted to the gas nitriding process, a general equation is obtained that controls the coefficients of each process of development of the kinetic parameter of the growth of *i*-th phase, the so-called constant of the parabolic growth of *i*-th phase, and other coefficients of the diffusion process. The construction of a general equation for the parameters of this process allows us to determine the diffusion coefficients of a single-phase and the development of the phase-in time. The equation describes the direct relationship of the phase's dynamic parameters with the difference in the phase boundary and the phase diffusion coefficient. However, this model does not consider the influence of temperature but depends only on the distribution of the concentration over the depth of the layer.

In a paper [32], the fundamentals of the model were presented and discussed, including the kinetics of compound layer growth and the determination of the nitrogen diffusivity in the diffusion zone. The nitrogen diffusivity in the diffusion zone is determined to be constant and only depends on the nitriding temperature, which is ~5×10^{-9} cm^2/s at 548 °C. However, the paper does not consider the issue of temperature distribution over the depth of the layer. There are no data on the adequacy of the model for varying the nitriding temperature.

In the study [33], the diffusion processes occurring during nitriding with FE methods are modeled. Nitriding of gas as a diffusion process was described by a differential equation, namely Fick's second law. This equation was solved with the Finite Element (FE) method. Modeling was based on the Orowan strengthening theory and the classic Johnson–Mehl–Avrami theory of precipitation.

The mathematical model of the diffusion processes of gas nitriding obtained in the present work does not contradict the existing and generally accepted models but complements the knowledge about the temperature distribution over the layer depth with the possibility of varying the temperature range of treatment. Thanks to the obtained model, it is possible to obtain data on the formation of the diffusion layer not only for the classical nitriding temperature (500–560 °C), but also for a lower nitriding temperature (for example, 450 °C), and a higher nitriding temperature (for example, 650 °C). All of this makes it possible to expand the knowledge about the features of the formation of the diffusion layer during the hardening of the surface of the part by gas nitriding.

As a result of the conducted studies, data on the distribution of temperature over the product's depth at different values of the exposure temperature necessary for predicting diffusion processes were obtained.

4. Conclusions

The dependence of the influence of the technological parameters of the chemical-heat treatment processes on the formation of the depth of the diffusion layers of steels and alloys is obtained. It is shown that mathematical modeling is advisable for solving a number of technological issues (e.g., determining and predicting the depth of the diffusion layer to determine specific gas nitriding conditions based on a given depth of the diffusion layer of steel). The relevance of obtaining mathematical models is associated with the technological and economic complexity of conducting a large number of experiments, as well as the need to know the dependencies of the influence of technological parameters of chemical and thermal treatment processes on the formation of the depth of the diffusion layers of steels and alloys.

As a result of modeling diffusion processes and experimental studies, data on the temperature distribution over the depth of the product at different values of the exposure temperature were obtained. Analytical methods made it possible to obtain functional dependencies for the temperature distribution over the depth of the layer and analyze the influence of various factors on the body's temperature state. The error of the obtained theoretical and experimental data does not exceed 3–5%. The results of the research can be used in production and scientific research.

Author Contributions: Conceptualization, K.K.; methodology, K.K., V.K., and V.I.; software, M.H., and D.D.; validation, I.P., M.H., and D.D.; formal analysis, K.K., V.I., and V.K.; investigation, K.K., V.I., and V.K.; resources, I.P. and D.D.; data curation, V.K., and M.H.; writing—original draft preparation, K.K. and V.K.; writing—review and editing, V.I. and M.H., visualization, V.K. and I.P.; supervision, V.I.; project administration, M.H.; funding acquisition, M.H. All authors have read and agreed to the published version of the manuscript.

Funding: The research was supported by research grant VEGA 1/0080/20 and KEGA 014TUKE-4/2020.

Institutional Review Board Statement: Not applicable.

Informed Consent Statement: Not applicable.

Acknowledgments: The research was partially supported by International Association for Technological Development and Innovations. The article is the result of the Project implementation: University Science Park TECHNICOM for Innovation Applications Supported by Knowledge Technology, ITMS: 26220220182, supported by the Research & Development Operational Programme funded by the ERDF.

Conflicts of Interest: The authors declare no conflict of interest.

References

1. Stetsko, A.E.; Stetsko, Y.T. Formation of Composite Reinforced Coating by Chemical Deposition and Chemical-Thermal Treatment of Boron and Carbon. *Microstruct. Prop. Micro Nanoscale Mater. Film. Coat.* **2020**, *240*, 261–270. [CrossRef]
2. Pashechko, M.; Józwik, J.; Dziedzic, K.; Karolus, M.; Usydus, I. Surface hardening of HS6-5-2 quick-cutting steel in the course of chemical thermal treatment. *Mater. Sci.* **2017**, *52*, 834–840. [CrossRef]

3. Mei, S.Q.; Guryev, A.M.; Ivanov, S.G.; Lygdenov, B.D.; Tsydypov, B.S.; He, X.Z.; Liang, Q.Y. Research on the chance of increasing the wear resistance of high-speed steel Using chemical thermal treatment methods. *IOP Conf. Ser. Mater. Sci. Eng.* **2019**, *479*. [CrossRef]
4. Fedorova, L.V.; Fedorov, S.K.; Serzhant, A.A.; Golovin, V.V.; Systerov, S.V. Electromechanical surface hardening of tubing steels. *Met. Sci. Heat Treat.* **2017**, *59*, 173–175. [CrossRef]
5. Ropyak, L.Y.; Shatskyi, I.P.; Makoviichuk, M.V. Analysis of interaction of thin coating with an abrasive using one-dimensional model. *Noveishie Tekhnol.* **2019**, *41*, 647–654. [CrossRef]
6. Yang, Y.; Yan, M.F.; Zhang, S.D.; Guo, J.H.; Jiang, S.S.; Li, D.Y. Diffusion behavior of carbon and its hardening effect on plasma carburized M50NiL steel: Influences of treatment temperature and duration. *Surf. Coat. Technol.* **2018**, *333*, 96–103. [CrossRef]
7. Marinin, E.; Gavrilov, G.; Belashova, I. The laser-plasma cementation as a method of increasing the abrasive resistance of medium-alloy tool steels. *Mater. Sci. Eng.* **2020**, *09*. [CrossRef]
8. Srivastava, S.; Snellings, R.; Meynen, V.; Cool, P. Utilising the principles of FeCO3 scaling for cementation in H2O-CO2 (g)-Fe system. *Corros. Sci.* **2020**, *169*, 108613. [CrossRef]
9. Che, H.L.; Tong, S.; Wang, K.S.; Lei, M.K.; Somers, M.A. Co-existence of γ′N phase and γN phase on nitrided austenitic Fe–Cr–Ni alloys-I. *experiment. Acta Mater.* **2019**, *177*, 35–45. [CrossRef]
10. Moskalioviene, T.; Galdikas, A. Kinetic model of anisotropic stress assisted diffusion of nitrogen in nitrided austenitic stainless steel. *Surf. Coat. Technol.* **2019**, *366*, 277–285. [CrossRef]
11. Kusmanov, S.A.; Silkin, S.A.; Belkin, P.N. Effect of Plasma-Electrolytic Polishing on the Corrosion Resistance of Structural Steels after Their Anodic Saturation with Nitrogen, Boron, and Carbon. *Russ. J. Electrochem.* **2020**, *56*, 356–364. [CrossRef]
12. Kostyk, V.O.; Kostyk, K.O.; Kovalov, V.D.; Turmanidze, R.; Dašić, P. Increase of operational properties of tools and machine parts nitriding the powder mixture. *Mater. Sci. Eng.* **2019**, *568*. [CrossRef]
13. Dong, J.; Liu, C.; Liu, Y.; Li, C.; Guo, Q.; Li, H. Effects of two different types of MX carbonitrides on austenite growth behavior of Nb-V-Ti microalloyed ultra-high strength steel. *Fusion Eng. Des.* **2017**, *125*, 415–422. [CrossRef]
14. Ivanov, I.V.; Mohylenets, M.V.; Dumenko, K.A.; Kryvchyk, L.; Khokhlova, T.S.; Pinchuk, V.L. Carbonitration of a tool for pressing stainless steel pipes. *J. Eng. Sci.* **2020**, *7*, 17–21. Available online: https://essuir.sumdu.edu.ua/handle/123456789/80836 (accessed on 12 March 2021).
15. Jain, N.; Singh, V.K.; Chauhan, S. Review on effect of chemical, thermal, additive treatment on mechanical properties of basalt fiber and their composites. *J. Mech. Behav. Mater.* **2017**, *26*, 205–211. [CrossRef]
16. Strugatsky, M.; Seleznyova, K.; Zubov, V.; Kliava, J. New insight in the nature of surface magnetic anisotropy in iron borate. *Surf. Sci.* **2018**, *668*, 80–84. [CrossRef]
17. Asayama, Y.; Hiyama, M.; Nakayama, T. Ionization and diffusion of metal atoms under electric field at metal/insulator interfaces; First-principles study. *Mater. Sci. Semicond. Process.* **2017**, *70*, 78–82. [CrossRef]
18. Zhong, J.; Chen, L.; Zhang, L. High-throughput determination of high-quality interdiffusion coefficients in metallic solids: A review. *J. Mater. Sci.* **2020**, *55*, 10303–10338. [CrossRef]
19. Ladianov, V.I.; Gilmutdinov, F.Z.; Nikonova, R.M.; Kashapov, N.F.; Shaekhov, M.F.; Khristoliubova, V.I. Effects of low pressure radio frequency discharge on the physical and mechanical characteristics and chemical composition of diffusion coating on a surface of complex configuration details. *IOP Conf. Ser. J. Phys. Conf. Ser.* **2017**, *789*. [CrossRef]
20. Khalaf Mohanad, M.; Kostyk, V.; Demin, D.; Kostyk, K. Modeling of the case depth and surface hardness of steel during ion nitriding. *East. Eur. J. Enterp. Technol.* **2016**, *2*, 80. [CrossRef]
21. Kostyuk, G.; Popov, V.; Kostyk, K. Computer Modeling of the Obtaining Nanostructures Process under the Action of Laser Radiation on Steel. *CMIS* **2019**, 729–743. Available online: http://ceur-ws.org/Vol-2353/paper58.pdf (accessed on 12 March 2021).
22. Gheiratmand, T.; Hosseini, H.M. Finemet nanocrystalline soft magnetic alloy: Investigation of glass forming ability, crystallization mechanism, production techniques, magnetic softness and the effect of replacing the main constituents by other elements. *J. Magn. Magn. Mater.* **2016**, *408*, 177–192. [CrossRef]
23. Poirier, D.R.; Geiger, G.H. *Transport Phenomena in Materials Processing*; Springer: Cham, Swizterland, 2016. [CrossRef]
24. Yang, X.; Zhang, Y. Prediction of high-entropy stabilized solid-solution in multi-component alloys. *Mater. Chem. Phys.* **2012**, *132*, 233–238. [CrossRef]
25. Singaravelu, D.L.; Vijay, R.; Filip, P. Influence of various cashew friction dusts on the fade and recovery characteristics of non-asbestos copper free brake friction composites. *Wear* **2019**, *426*, 1129–1141. [CrossRef]
26. Guo, S.; Hu, Q.; Ng, C.; Liu, C.T. More than entropy in high-entropy alloys: Forming solid solutions or amorphous phase. *Intermetallics* **2013**, *41*, 96–103. [CrossRef]
27. Gavriljuk, V.G. Carbon, Nitrogen and Hydrogen in Iron-Based Solid Solutions: Similarities and Differences in their Effect on Structure and Properties. *Met. Noveishye Tekhnolohyy* **2016**, *38*, 67. [CrossRef]
28. Siyahjani, F.; Atar, E.; Cimenoglu, H. Structural changes on the surface of alloy Ti6Al7Nb under gas nitriding. *Met. Sci. Heat Treat.* **2016**, *5*, 170–174. [CrossRef]
29. Jones, R.; Goss, J.P.; Pinto, H.; Palmer, D.W. Diffusion of nitrogen in diamond and the formation of A-centres. *Diam. Relat. Mater.* **2015**, *53*, 35–39. [CrossRef]
30. Dhafer, W.A.R.; Kostyk, V.; Kostyk, K.; Glotka, A.; Chechel, M. The choice of the optimal temperature and time parameters of gas nitriding of steel. *East. Eur. J. Enterp. Technol.* **2016**, *3*, 44–50. [CrossRef]

31. Nam, N.D.; Xuan, N.A.; Van Bach, N.; Nhung, L.T.; Chieu, L.T. Control gas nitriding process: A review. *J. Mech. Eng. Res. Dev.* **2019**, *42*, 17–25. [CrossRef]
32. Yang, M.; Zimmerman, C.; Donahue, D.; Sisson, R.D. Modeling the Gas Nitriding Process of Low Alloy Steels. *J. Mater. Eng. Perform.* **2012**, *22*, 1892–1898. [CrossRef]
33. Syla, N.; Elezaj, N.; Aliaj, F.; Tolaj, Z.; Zeqiraj, A. Finite element modeling of 31CrMoV9 steel hardness curves after gas nitriding. *Indian J. Chem. Technol.* **2019**, *26*, 358–361. Available online: http://nopr.niscair.res.in/handle/123456789/49683 (accessed on 12 March 2021).